Non-free ionic transport of sodium, magnesium, and calcium in streams of two adjacent headwater catchments with different vegetation types in Japan

AUTHOR(S):

Terajima, Tomomi; Moriizumi, Mihoko; Nakamura, Tomohiro

CITATION:

Terajima, Tomomi ...[et al]. Non-free ionic transport of sodium, magnesium, and calcium in streams of two adjacent headwater catchments with different vegetation types in Japan. Journal of Hydrology 2017, 544: 58-73

ISSUE DATE:

2017-01

URL:

http://hdl.handle.net/2433/230281

Non-free ionic transport of sodium, magnesium, and calcium in streams of two adjacent headwater catchments with different vegetation types in Japan

Tomomi TERAJIMA[*a], Mihoko MORIIZUMI[*b], and Tomohiro NAKAMURA[*c]

*a: Disaster Prevention Research Institute, Kyoto University. Gokasho, Uji, Kyoto 611-0011, Japan; terajima@scs.dpri.kyoto-u.ac.jp

*b: Faculty of Agriculture, Ryukoku University. 1-5, Yokoya, Seta-Ohecho, Otsu, Shiga 520-2194, Japan; moriizu@agr.ryukoku.ac.jp

*c: Suuri-Keikaku Co. Ltd. 2-5-4 Sarugaku-cho, Chiyoda, Tokyo 101-0064, Japan; nakamura_tomohiro@sur.co.jp

Corresponding author: T. Terajima

Tel: +81-774-38-4628

Fax: +81-774-38-4118

E-mail address: terajima@scs.dpri.kyoto-u.ac.jp

SUMMARY

Sodium (Na), magnesium (Mg), calcium (Ca) are usually believed to occur mostly as free ions in the fresh water and consequently little is known about their chemical species. To understand the importance of non-free ionic fractions (NIF) of major metals in freshwater streams, Na, Mg, Ca, silicon (Si), and fulvic acid-like materials (FAM) were measured in streams of mountainous adjacent headwater catchments

dominated by different vegetation types (planted evergreen coniferous forest and natural deciduous broadleaf forest). During both no rainfall periods and rainstorms, the proportion of NIF relative to total elements was lower in the coniferous catchment than in the deciduous catchment, although it sometimes accounted for half or more of the total concentrations of Na, Mg, and Ca in both catchments. The solubility of metal compounds was higher than the measured maximum concentrations of Na^{+}, Mg^{2+}, and Ca^{2+} to the extent that inorganic bonding was hardly possible. During no rainfall periods when FAM was slightly produced into the streams, the fluxes of NIF and Si were highly correlated ($r > 0.92$, $p < 0.0001$, $n = 30$) in both catchments. During a small rainstorm, the flux of NIF correlated weakly with that of Si but did not correlate with that of FAM in both catchments. In contrast, during a heavy rainstorm, the flux of NIF correlated strongly ($r \geq 0.83$, $p < 0.0001$, $n = 26$) with that of FAM in the deciduous catchment where relatively deep soil water compared to near-surface water was the predominant component of stream water. However, during the heavy rainstorm in the coniferous catchment, only the flux of NIF originated in the quick-flow component (i.e., surface or near-surface water) in stream water (ΔNIF) correlated strongly ($r \geq 0.81$, $p < 0.0001$, $n = 22$) with that of FAM. These findings imply that heavy rainstorms may enhance the bonding of the major metals with humic substances mainly in the deciduous catchment; and also exhibit that, in the headwater catchments, both water flow pathways resulted from the different vegetation types play a very important role to promote the bonding of major metals with humic substances in stream water.

Key words: fulvic acid, major metal, bonding, humic substance, organic–inorganic interaction

1. Introduction

Major metals such as sodium (Na), magnesium (Mg), and calcium (Ca), which are the vital elements involving the metabolism and physiological function of life, are thought to occur mainly (> 98%) as free ions in freshwater environments (e.g., Mantoura *et al*., 1978). On the contrary, the biogeochemical implication (i.e., bonding) of the major metals, humic substances, and nano-scale phyllosilicates represented by clay minerals (Wilson *et al*., 2008) has been mentioned in particular in the laboratory and modeling studies (e.g., Choppin and Shanbhag, 1981; Livens, 1991; Romkens *et al.*, 1996; Majzik, A. and Tombacz, E., 2007; Takahashi *et al.*, 1999 and 2002). This discrepancy regarding major metal species implies that little is known about their transport forms (i.e., chemical species) in freshwater environments.

In contrast, as described by Tipping (1993), the information regarding the effect of environmental factors (topography, geology, climate, hydrology, vegetation, etc.) on metal bonding must be very useful to allow the calculation and modeling of chemical speciation under natural condition in freshwater environments. Furthermore, the insights related to the interaction between aquatic and terrestrial biogeochemistry will also facilitate a better understanding of controls on humic substance production, consumption, and flux across whole landscapes and biomes (McDowell, 2003). However, the effects of environmental factors on bonding possibility of major metals to humic substances and nano-scale phyllosilicates and consequently the transport in

bonding in stream water are as yet unclear.

Accordingly, characterizing the bonding of major metals to humic substances and nano-scale phyllosilicates in field sites must provide useful information about the chemical regimes in stream catchments, and besides, give a novel knowledge in catchment hydrology. If the free ions of major metals combined with humic substances and nano-scale phyllosilicates, the relationships between the fluxes of combined materials (i.e., non-free ionic fraction of the major metals), humic substances, and nano-scale phyllosilicates can be the good indices to explore broadly both the implication as represented by the bonding of Na, Mg, and Ca and consequently the characteristics of bonding resulted from the environmental factors.

Thus we measured Na, Mg, Ca, and silicon (Si) in streams of two mountainous adjacent headwater catchments composed of differing vegetation. Fulvic acid-like materials (FAM), representative of dissolved organic matter (DOM) in the streams that we observed (Terajima and Moriizumi, 2013) and usually accounts for 60% to 99% of DOM in stream or ground water (Thurman, 1985; Malcolm, 1990; Artinger *et al.*, 2000), were also measured to understand the interaction among the major metals, clay minerals, and humic substances. Additionally, FAM and dissolved organic carbon (DOC) was measured for soil extracts from both catchments to determine where FAM and DOC are stored in the soil profile and examine water flow pathways along the slopes. Subsequently we broadly estimated how stream water chemistry (i.e., bonding possibility) was provided and how slope hydrology depending on differing vegetation (i.e., environmental factor) affected the transport of major metals.

2. Site description

2.1. Topography, geology, and climate

The study area consisted of two mountainous headwater catchments with differing vegetation in the Nariki catchment (35˚50′N and 139˚10′E at the rain gauge in Fig. 1a), which is about 40 km west of central Tokyo. Slope gradients in the catchment range between 35° and 45°, and Mt. Kuro-yama, at 842 m, is the highest point. The catchment is underlain by sandstone and mudstone bedrock of Jurassic age that also contains some chert. The rock layers dip 60 - 90° northeast and strike NW-SE (Inosato *et al.*, 1980; Tokyo Prefectural Public Work Institute, 2002).

According to data from the Automated Meteorological Data Acquisition System (AMeDAS) of the Japan Meteorological Agency, the average annual precipitation between 1976 and 2009 at Ohme city (35°47′N, 139°18′E; 10 km southeast of the Nariki catchment and 100 m in elevation) was 1487 mm, and the average minimum, maximum, and annual air temperatures during the same period were –6.7 °C in late January, 36.9 °C in mid-August, and 14.2 °C, respectively. Rainstorms occur mainly from mid-June to late July (the rainy season), and in the typhoon season which lasts from mid-August to mid-October. About 80% of the annual precipitation falls during these periods. Dry conditions prevail in winter, from early December to early March, although snow usually accumulates in the Nariki catchment to a maximum depth of 10 to 20 cm in February. The stream water temperature of both headwater catchments ranged from 10 °C in winter to 23 °C in summer.

2.2. Experimental catchments

A first headwater stream (first-order stream; 70 m in length) on the north side of the Nariki River (Figs. 1a and 1b) is densely surrounded by an unmanaged evergreen coniferous forest composed of Japanese cedar (*Cryptomeria japonica*) and Hinoki cypress (*Chamaecyparis obtusa*) which were planted in 1961 (Coniferous catchment: 1.29 ha, 100 m in relief; Fig. 2a). In 2007, the catchment contained 2000 to 2500 trees ha^{-1}, most with trunk diameters of $\leq$ 20 cm. The forest canopy is mostly closed, with little understory vegetation owing to the weak penetration of sunlight to the forest floor. The litter layer on the forest floor is very thin, and mineral soil is exposed in some places.

A second headwater stream (first-order stream; 70 m in length) on the south side of the Nariki River (Fig. 1a and 1c) is surrounded by a natural deciduous broadleaf forest (Deciduous catchment: 1.28 ha, 100 m in relief; Fig. 2b). The dominant tree species in this catchment are oak (*Quercus serrata* and *Quercus mongolica*), beech (*Fagus japonica*), chestnut (*Castanea crenatus*), and Japanese maple (*Acer palmatum*). The understory vegetation is dense in comparison to that in the coniferous catchment, and there is a thick litter layer on the forest floor.

The riparian zone (the flat bottomland along the streams) is very small and narrow in both catchments (Figs. 1b and 1c). Thus the contribution of subsurface and groundwater flow for the stream water generation, which had been involved in the riparian zone before rainstorms, seems to be relatively small compared to those from the slopes.

The boundary between soil and bedrock was determined by cone penetration test to occur at N_{10} = 50, and the soil depth ($N_{10} \leq 50$) in both catchments was $\leq$ 3 m. The

structure of the soil profile (the soil horizons present and their thicknesses) is similar along the slopes of both catchments. In both catchments, the soils are classified as Cambisols (according to the classification by the Food and Agriculture Organization of the United Nations), and soil pH ranges between 3.8 and 5.2 throughout the vertical soil profile in both catchments. The strongly organic-rich soil horizons, the A_0 to AB horizons, are up to 25 cm thick in both catchments, and a gravel rich mineral soil (B horizon) is below 15 to 25 cm depth. The soil parent material is presumably derived from upslope via soil creep or rock slides because many discrete angular stones and sediment particles in various size are included and mixed intricately throughout the soil profiles. The saturation hydraulic conductivity (K_{sat}) of the soil above 80 cm depth in both catchments ranges mostly between 10^{-2} and 10^{-3} cm s^{-1}. Soil porosity in the coniferous catchment gradually decreases with soil depth, ranging between 70% at 10 cm depth and 45% at 70 cm depth, whereas soil porosity in the deciduous catchment is relatively constant, decreasing from 70% near the soil surface to 53% at 70 cm depth. The gravitational water drainage capacity of the soil in the coniferous catchment is below 5%, except between 0 and 5 cm depth, where it is 28%. In the deciduous catchment, it is constant at 9% throughout the soil profile up to 50 cm depth (Hirano *et al.*, 2008).

A unique high permeable and organic rich layer, the so-called biomat ($Ks > 10^{-2}$ cm s^{-1}; porosity above 70%), consisting of a dense network of fine roots of Japanese cedar and Hinoki cypress within the loose litter and root-permeated zone (Sidle *et al.*, 2007), was common on the slope surface (above 0 cm depth) in the coniferous catchment. Its thickness varied from a few centimeters to 20 cm in the coniferous catchment, but it

was rare in the deciduous catchment (Terajima and Moriizumi, 2013). Thus water flow through the biomat (i.e., biomatflow) during rainstorms appeared predominantly in the coniferous catchment (Hirano *et al.*, 2008).

On the basis of the above facts, the characteristics of the environmental factors in the two headwater catchments are briefly summarized as follows: The same or similar characteristics are geography, topography (i.e., catchment area, elevation, relief, slope, stream order, and stream length), geology, soil (i.e., type and depth), and climate. In contrast, the different characteristics are vegetation, soil profile (i.e., biomat and little litter layer predominant in the coniferous catchment), and resultantly hillslope hydrology (i.e., biomatflow predominant in the coniferous catchment).

3. Instrumentation and data collection

3.1. Soil collection and soil water extraction

We collected soil samples at slope surfaces and at 20 to 30 cm intervals up to 140 cm depth (within the limits of the possible to excavate manually) at the ridgetop, mid-, and lower slopes in both catchments.

The collected soil samples (soil pH ranged between 3.8 and 5.2) were air-dried and subsequently 3 g of the samples were shaken for 24 h in 60 mL of ultrapure water (pH 5.6, 18.2 MΩ cm, and dissolved organic carbon (DOC) < 0.01 μg L^{-1}) obtained from an Advantec Japan ® water purification system (model number: RFU585DA). Then, the soil extracts were filtered for the measurements of excitation-emission matrix fluorescence spectrum (EEM spectrum) and DOC to obtain the information on the storage of water extractable FAM and DOC in soil. The EEM analysis for soil extracts

is described in Section *3.4.4*. The DOC concentration was measured with a Shimadzu ® organic carbon analyzer (model number: TOC-V; Detection limit is 0.004 mg $L^{-1}$and measurement error was ≤ ± 0.075 mg L^{-1}).

The absolute values of the EEM spectrum in soil extracts are variable on account of the measurement method based on the proportion of air-dried soil weight relative to ultrapure water volume. Thus, the values of EEM spectrum in soil extracts are impossible to compare directly with those in stream water.

3.2. Measurement of rainfall and stream discharge

A rain gauge (0.2 mm $count^{-1}$), which recorded precipitation at 5-min intervals, was installed in an open space near the two catchments (710 m elevation; Fig. 1a) where rainfall was unlikely to be intercepted by the tree canopies because of no canopies beyond 45° in elevation. According to our past study (Nogi, 2007; unpublished), the average annual rainfall interception by the tree canopy was about 18% and 16% of total rainfall in the coniferous and deciduous catchments, respectively. Moreover, the concentration of Na^+, Mg^{2+}, and Ca^{2+} supplied by rainfall (through fall + stem flow) into the forests in both catchments differed by < 1.0 mg L^{-1}. These things imply that the flux of Na^+, Mg^{2+}, and Ca^{2+} into the forests was < 4.66×10^{-2} mg s^{-1} and < 4.98×10^{-2} mg s^{-1} in the coniferous and deciduous catchments, respectively; mostly similar in both catchments. In contrast, the flux of potassium ions (K^+) into the forests in the coniferous catchment was 50% of that in the deciduous catchment.

Stream discharge in the two catchments was measured from January 2006 to September 2007 using parshall flumes (15 cm size) installed at the lower end of the

streams in both catchments (Figs. 1b and 1c). Water levels in the flumes were recorded at 5-min intervals by a Trutrack ® automatic sensors (model number: WT-HR64K), and the relationship between the water level and the stream discharge manually measured at the flumes, the H-Q relation, was used to estimate the specific stream discharge ($m^3d^{-1}ha^{-1}$ or $L\ s^{-1}ha^{-1}$) throughout the observation period.

3.3. Stream water collection

Quick-flow component in stream water is very difficult to quantify immediately in field sites. Thus in our study, notwithstanding the time intervals after rainstorms, the baseflow situation was qualitatively defined as when the hydrograph was on the falling limb and stream discharge seemed to be small and constant even though the small rainfall was supplied; implying when the quick-flow component seemed not to contribute directly to stream discharge (i.e., no increase in stream discharge).

Stream water during no rainfall periods (baseflow) in both catchments was manually and randomly collected in polyethylene bottles from January 2006 to August 2007 (total numbers of baseflow samples in both catchments were 54, but were 30 for collection from October 2006 to August 2007). The minimum and maximum stream discharge (i.e., baseflow discharge in this case) at collection were 0.02 $L\ s^{-1}\ ha^{-1}$ (8 May 2006) and 3.19 $L\ s^{-1}\ ha^{-1}$ (8 October 2006) in the coniferous catchment, and 0.53 $L\ s^{-1}\ ha^{-1}$ (23 March 2006) and 5.06 $L\ s^{-1}\ ha^{-1}$ (8 October 2006) in the deciduous catchment, respectively.

Two rainstorms (Storm 1 and Storm 2, 26 to 27 September 2006 and 14 to 16 July 2007, respectively) caused increased stream water. Flow samples were collected during

these storms in polyethylene bottles by at 60 to 90 min intervals through an American SIGMA ® water samplers (model number: 900) on the upstream side of the partial flumes. The numbers of water samples in both catchments were 24 and 29 for Storm 1 and Storm 2, respectively. Storm 1 had a small-scale rainstorm with 40.4 mm of total rainfall, maximum rainfall intensity of 1.9 mm 5 min^{-1}, and 8.2 days yr^{-1} in rainfall frequency for the same storm scale. In contrast, Storm 2 was a typhoon storm with 117.0 mm of total rainfall, maximum rainfall intensity of 1.6 mm 5 min^{-1}, and 2.9 days yr^{-1} in rainfall frequency for the same storm scale.

Glass bottles were also used for intermittent manual sampling of the stream water during no rainfall periods and rainstorms to verify the effect of chemical adsorption caused by the difference in collection materials. The concentration of major metals and EEM spectrum of stream water was then compared with those of the water samples collected simultaneously in the polyethylene bottles; they were below measurement errors for total elements and ionic materials described in Sections *3.4.1.* and *3.4.2.* and < 0.13 QSU for FAM. This finding implies that no influence to the concentration of major metals and the EEM spectra of samples was brought by the difference in collection materials.

Water samples collected in polyethylene bottles were transferred to glass bottles as soon as possible. The samples during no rainfall periods were stored at 4 °C within one day after collection, whereas the samples during rainstorms were stored within 3 days after collection, because the water collection during rainstorms ran for 2 or 3 days. All stream water samples were filtered within 5 days (120 hrs,) after collection. The 0.45-μm mixed cellulose ester filters (Advantec Japan or Sartorius Mechatronics

Japan) were used in the filtration. Then analyses were conducted for total elements (T-Na, T-Mg, T-Ca, and T-Si), free ions (Na^+, Mg^{2+}, and Ca^{2+}; K^+ was scarcely detected in the stream water), and EEM spectra.

3.4. Measurement of concentrations in water samples

3.4.1. Total elements (T-Na, T-Mg, T-Ca, and T-Si)

At first, 5 mL of hydrochloric acid (HCl: 3 mol L^{-1}) was added to 40 mL of filtered water to obtain the high sensitivity for the measurement of major metals by adjusting the pH between 0.5 and 1.0, the approximate pH of standard solutions for the major metals of an inductively coupled plasma atomic emission spectrometer (ICP) that we used. A Shimadzu ® ICP (model number: ICPS-1000 IV, Detection limit is 0.01 mg L^{-1}) was used to measure the concentration of total elements in the filtrate. The injection volume of water sample was 30 mL. Standard solutions for Na, Mg, Ca, and Si, of which the concentrations were 1, 5, and 25 mg L^{-1}, were used to calibrate the results (measurement errors: ≤ ± 0.01 mg L^{-1} for Na-, ≤ ± 0.04 mg L^{-1} for Mg-, ≤ ±0.17 mg L^{-1} for Ca-, and ≤ ± 0.01 mg L^{-1} for Si-analyses).

3.4.2. Free ions (Na^+, Mg^{2+}, and Ca^{2+})

Free ions in the stream water filtrate without added HCl were measured with a TOA-DKK ® ion chromatograph (IC; model number: IA-200 for anions and IA-300 for cations). The minimum injection volume of water sample into the instruments was 0.2 mL for anions and 0.02 mL for cations, measurement temperature was 40 ± 4˚C, and detection limit is 0.01 mg L^{-1}. The eluant (mixed solution of phthalic acid, tris

hydroxymethyl aminomethane, and boric acid for anions; and methane-sulfonic acid solution for cations) have a pH of 3.0. Single-point calibration by measurement of a standard solution of each ion (10 mg L^{-1} of Cl^-, NO_3^-, Na^+, and Mg^{2+}, and 20 mg L^{-1} of SO_4^{2-}, K^+, and Ca^{2+}) was used (measurement errors: ≤ ± 0.1 mg L^{-1}). Bicarbonate (HCO_3^-) was measured by the titration for the stream water samples of 50 mL, which was calculated from the alkalinity under pH=4.8 (measurement error: ≤ ± 0.3 mg L^{-1}).

The pH of the stream water during the observation period ranged between 6.0 and 8.0. Thus, the concentrations of ions measured by IC with an eluant pH of 3.0 may have been somewhat higher than their natural concentrations in the stream water. Although we didn't quantify the concentration of organic acid (OA), chromatic peaks likely to be the formic acid and oxalic acid were detected mainly in water samples from the coniferous catchment.

3.4.3. Non-free ionic fraction (NIF)

Strellis *et al*. (1996) indicated that laboratory standard calibration was the most likely sources of large systematic errors in ICP and IC analyses. Thus, the concentrations of the standard solutions, used for each calibration for ICP and IC, were alternately measured with IC and ICP to identify and correct any instrumental discrepancies between ICP and IC analyses. Each measured concentration, however, ranged within the measurement error, implying that the measured concentrations were mostly same as the originals of each standard solution and consequently the instrumental discrepancies were negligible in our measurement.

The difference in concentration between total elements and free ions of metal

elements were equated with the concentration of non-free ionic fractions (NIF: all materials that were not measurable with IC).

3.4.4. Fulvic acid-like materials (FAM)

The EEM spectra in the filtrate for the soil extracts and stream water samples without added HCl were measured with a JASCO ® 3-dimensional EEM spectrometer (model number: FP-6600), at excitation wavelengths of 220–550 nm and emission wavelengths of 250–600 nm (i.e., Ex/Em: 220-550/250-600) and a scanning speed of 2000 nm min^{-1} (measurement error was ≤ ± 0.08 QSU). In our measurements (e.g., Fig. 3), a visible single peak in fluorescence intensity corresponding to FAM appeared in the water samples during rainstorms at around Ex/Em: 340/440 (Coble *et al*., 1993; Suzuki *et al*., 1998; Mostofa *et al*., 2005; Fellman *et al*., 2010), which could reflect the terrestrially organic matter derived from vascular plants or soil organic matter in wetlands and forested environment (Coble, 1996; Coble *et al*., 1998). Although another peak in fluorescence intensity appeared at around Ex/Em: 260/440 (Fig. 3c to 3f) corresponding to fluorescence that resembles fulvic acid (Fellman *et al*., 2010), we adopted exclusively the peaks at around Ex/Em: 340/440 for our analyses. In contrast, as shown in Fig. 3a and 3b, we did not measure FAM during no rainfall periods because visible fluorescent peaks did not always appear, so that no data is presented.

Irrespective of stream discharge during rainstorms, some stream water samples (2 and 5 samples for Storm 1 in the coniferous and deciduous catchments, respectively, and 10 samples for Storm 2 in both catchments) exhibited small peaks at around Ex/Em: 270/320 (< 2.4 QSU and < 1.3 QSU in the coniferous and deciduous

catchments, respectively), possibly corresponding to peaks in amino acid-like (or protein-like) materials (Coble *et al*., 1993; Fellman *et al*., 2010). As shown in Fig. 3, the peaks indicating humic acid-like (e.g., at around Ex/Em: 480/520) and other unknown materials were not detected visibly in our analyses.

To determine the fluorescence intensity of FAM (*F*-FAM), the peaks in fluorescence intensity corresponding to FAM were normalized relative to the fluorescence intensity of a 10 μg L^{-1} quinine sulfate solution (= 10 QSU) at Ex/Em: 345/440; close to the peak obtained for FAM (Ex/Em: 340/440). The solvent (sulfuric acid, 0.1 mol L^{-1}; Wako Pure Chemical Industries Japan) of this solution exhibited no fluorescence spectrum. The fluorescence intensity of the quinine sulfate solution was verified every 140 min (for every batch of seven water samples) to determine any instrumental errors which may have been caused by fluctuations in illumination.

In Terajima and Moriizumi (2013), the correlation lines of the *F*-FAM relative to DOC concentration showed the linear correlations with different slopes for each water sample at DOC < 22 mg L^{-1} and *F*-FAM < 120 QSU but became convex at DOC > 22 mg L^{-1} and *F*-FAM > 120 QSU. This shows that attenuation of the FAM spectrum due to high FAM concentration probably began at values > 120 QSU. *F*-FAM of the soil extracts from soil surfaces were greater than > 120 QSU (Fig. 4a). Thus the FAM spectrum of these samples (without dilution) could have been attenuated and consequently natural *F*-FAM of the soil extracts at soil surfaces may be greater than the data shown in Fig. 4a. In contrast, because the *F*-FAM of all stream water filtrate was < 20 QSU, we did not dilute the water samples to avoid FAM spectrum attenuation.

The *F*-FAM of water should usually be corrected for the inner filtering effect, for example, on the basis of Lakowicz (1999). However, the correction coefficients of the stream water filtrate, of which all *F*-FAM was below 20 QSU in our study, ranged within the measurement error of the fluorescence intensity of 10 μg L^{-1} quinine sulfate solution. Accordingly, except for the soil extracts, the inner filter correction of the stream water filtrate found to be negligible and thus we did not conduct the correction for stream water.

3.5. Statistical analysis

To understand roughly the bonding possibility of NIF in the headwater streams, we examined the relationship between stream discharge, the fluxes of Si, NIF, and FAM by calculating their linear correlation coefficients (*r*-values with *p*- and *n*-values) during no rainfall periods and two rainstorms. Then, total elements, free ions, NIF, and Si (all units are in [mg L^{-1}]) were multiplied by the specific stream discharge at corresponding water correction [L s^{-1} ha^{-1}] to obtain their specific fluxes [mg s^{-1} ha^{-1}]. In addition, to equivalently compare the relative differences in NIF transport affected by the FAM amount in the stream water of the coniferous and deciduous catchments, the *F*-FAM [QSU] (i.e., apparent concentration) was multiplied by the specific stream discharge at corresponding water collection [L s^{-1} ha^{-1}] and we obtained the apparent specific flux of FAM [QSU L s^{-1} ha^{-1}] in the stream water of both catchments.

Because the specific flux is obtained from multiplying the concentration of major metals by specific stream discharge, the relationship between the specific flux and specific stream discharge seems inevitably to show a good correlation. For example in

a headwater in Japan, however, the flux of wash load (i.e., multiplying the concentration of wash loads by stream discharge) does not always necessarily represent good correlations with stream discharge (Terajima *et al.*, 1997). Besides, the sources of stream water, major metals, Si, NIF, and FAM are surmised to be spatially and temporally different even in small headwater catchments: which seems too hard to understand the relationship between the complicated hydrological processes and the cause of changes in concentration. In addition, the specific flux is convenient both to compare the chemical characteristics in various streams where catchment area and stream discharge is usually different and to separate the flow component of stream water as described in Section *3.6*. Accordingly, in the strict sense, although the relationships between specific stream discharge, the specific flux of major metals, Si, NIF, and FAM do not necessary reveal the bonding forms of Na, Mg, and Ca in stream water, the specific flux (involving the difference in stream discharge and catchment area) can be one of the useful factors capable of understanding the transport dynamics based on the mass balance of chemical materials.

3.6. Separation of the stream water components and NIF

Hirano *et al.* (2009) suggested that in the catchments we observed, the Si concentration could be used as index for assessing the baseflow component of the stream water. The baseflow component of the stream water derives from groundwater or deep subsurface water, and as a result of reactions between the water and the soil or basement rocks during the relatively long contact time between them, the Si concentration in the baseflow is high (Wels *et al.*, 1991). Hirano *et al.* (2009) also

showed that, based on the mass conservation law and the Si flux, the baseflow component of the stream water during rainstorms could be calculated as follows:

$$Q_{\text{(baseflow in rainstorm)}} = Q_{\text{(rainstorm)}} (1 - Q_{\text{(quick-flow)}} / Q_{\text{(rainstorm)}}), \quad (1)$$

where $Q_{\text{(baseflow in rainstorm)}}$ is the baseflow component of the stream water during rainstorms; $Q_{\text{(rainstorm)}}$ is the measured stream discharge during rainstorms, including both baseflow and quick-flow components; and $Q_{\text{(quick-flow)}}$ is the quick-flow component of the stream water calculated from the Si flux of near-surface water, as represented by rainwater containing relatively low Si concentrations (a maximum of 0.27 mg L^{-1} in the presented case). Thus, in Eq. 1, $Q_{\text{(quick-flow)}} / Q_{\text{(rainstorm)}}$ is the ratio of the quick-flow component to the total stream discharge during rainstorms, and $(1 - Q_{\text{(quick-flow)}} / Q_{\text{(rainstorm)}})$ represents the ratio of the baseflow component to the total stream discharge during rainstorms. Both these ratios can change over the course of a storm.

The NIF flux originating from the quick-flow component of the stream water (ΔNIF) is calculated as follows:

$$\Delta NIF = NIF_{\text{(rainstorm)}} - NIF_{\text{(baseflow in rainstorm)}}, \quad (2)$$

where $NIF_{\text{(rainstorm)}}$ is the measured NIF flux in the stream water during rainstorms, including both the baseflow and quick-flow components; and $NIF_{\text{(baseflow in rainstorm)}}$ is the NIF flux derived from the baseflow component during rainstorms, of which the calculation will be presented in Section *5.3.1.* (i.e., Eq. 5). In Eq. 2, ΔNIF would be derived mostly from relatively shallow soils with high FAM (Fig. 4a) resulted from shallow subsurface and near-surface water as biomatflow.

On the basis of Eqs. 1 and 2, with combining the other Eqs. noted in the sections of *5.2.1* and *5.3.1* (i.e., Eqs. 3 to 6), NIF dynamics in stream water and bonding

possibility of the major metals with FAM and/or nano-scale phyllosilicates such as clay minerals will be discussed.

4. Results

4.1. FAM distribution in soil

The concentrations of water extractable FAM and DOC in soils in the coniferous and deciduous catchments are shown in Fig. 4. Regardless of the slope position, FAM (Fig. 4a) in the coniferous catchment occurred mainly in the shallow part of soil above 50 cm depth. In the deciduous catchment, higher FAM was measured at the mid and lower slope positions than at the ridge top, even below 50 cm depth. The distribution of DOC (Fig. 4b) was similar to that of FAM though the concentrations below 50 cm depth ranged between a few mg L^{-1} and 10 mg L^{-1} especially in the coniferous catchment.

4.2. Major metals and Si in stream water during no rainfall periods

We examined the changes in stream water chemistry and the proportion of NIF relative to total elements in stream water (baseflow) during no rainfall periods from 2006 to 2007 (Fig. 5). The pH of the stream water ranged between 6.0 and 7.0 in both catchments, however, that of the baseflow during the summer season tended to have been 0.5 - 1.0 pH units higher than that during the winter season in both catchments.

Fig. 5 shows that, except for the concentrations of T-Ca and Ca^{2+} in the coniferous catchment, which respectively ranged from 6 to 10 mg L^{-1} and from 5 to 8 mg L^{-1}, the concentrations of the total elements (T-Na, -Mg, and -Ca) and free ions (Na^{+}, Mg^{2+},

and Ca^{2+}) were mostly below 5 mg L^{-1} in both catchments.

The concentrations of total elements were higher in the coniferous catchment than in the deciduous catchment throughout the observation period. In addition, Fig. 6 shows that the flow chemistry in free ions showed the Ca-HCO_3 type in both catchments. Although the concentration of free ions tended to rise through winter into summer in both catchments, it was higher in the coniferous catchment than in the deciduous catchment (i.e., mean concentrations were 1.4, 0.4, and 3.6 mg L^{-1} higher for T-Na, T-Mg, and T-Ca, respectively; and 1.4, 0.4, and 3.6 mg L^{-1} higher for Na^{+}, Mg^{2+}, and Ca^{2+}, respectively).

The mean Si concentration was 6.22 mg L^{-1} in the coniferous catchment and 4.88 mg L^{-1} in the deciduous catchment, 1.3 times higher on average in the coniferous catchment than in the deciduous catchment. However, because the stream discharge (i.e., baseflow in this case) in the coniferous catchment was about 0.7 - 0.8 times less on average than that in the deciduous catchment, the specific fluxes of Si were eventually similar in the two catchments throughout the observation period.

The proportion of NIF relative to total element ranged from 0.6% to 40.0% in the coniferous catchment and from 7.3% to 58.0% in the deciduous catchments (refer to no rainfall periods in Table 1a). They tended to become lower (7% to 19 % on average) after May 2007 except during rainfall periods and NIF-Ca in the deciduous catchment (Fig. 5), resulting from the rise of concentration of free ions relative to total elements through winter into summer as shown in Fig. 6. In addition, the proportions of NIF in the coniferous catchment (Table 1a) were 13.6% (in NIF-Na), 11.3% (in NIF-Mg), and 25.4% (in NIF-Ca) lower on average, with a significant difference under all $p < 0.0001$

and n = 30, than those in the deciduous catchment. Thus in the stream water during no rainfall periods, although the concentrations of total elements and free ions were mostly higher in the coniferous catchment than in the deciduous catchment, the proportion of NIF in the stream water were less in the coniferous catchment than in the deciduous catchment.

4.3. Major metals, Si, and FAM in stream water during rainstorms

We next examined the changes in stream water chemistry and the proportion of NIF relative to total elements during rainstorms. The changes in pH of low and peak stream discharge during the rainstorms in the two catchments were from 6.0 to 7.5. The result in Storm 2 (a typhoon storm with total rainfall of 117 mm) is specifically shown in Fig. 7. In the coniferous catchment, stream discharge initially peaked at 2.5 L s^{-1} ha^{-1} at 00:00 LT on 15 July and peaked a second time at 8.5 L s^{-1} ha^{-1} at 12:30 LT on 15 July. In contrast, in the deciduous catchment, the stream discharge during the morning of 15 July was about 1 L s^{-1} ha^{-1} without clear peak, but a peak of 8.0 L s^{-1} ha^{-1}, similar in amount to the second peak in the coniferous catchment, occurred at 12:30 LT on 15 July.

T-Na and Na^+ concentrations in the coniferous catchment were relatively about 1.0 and 1.4 mg L^{-1} higher on average than those in the deciduous catchment. However, T-Mg and Mg^{2+} concentrations were almost the same in both catchments: same on average in T-Mg and 0.2 mg L^{-1} higher on average in Mg^{2+} in the coniferous catchment than in the deciduous catchment. In contrast, T-Ca concentrations were similar in both catchments (0.18 mg L^{-1} lower on average in the coniferous catchment than in the

deciduous catchment), whereas Ca^{2+} concentrations in the coniferous catchment were about 1.7 mg L^{-1} higher on average than those in the deciduous catchment. These facts provide that the NIF-Ca concentration (ratio) in the coniferous catchment was consequently lower than that in the deciduous catchment.

The mean Si concentration in the coniferous catchment was 6.09 mg L^{-1} and that in the deciduous catchment was 3.50 mg L^{-1}, 2.59 mg L^{-1} higher in the coniferous catchment than in the deciduous catchment. This difference in concentrations resulted in higher Si fluxes in the coniferous catchment than in the deciduous catchment during Storm 2, because stream discharge was similar for the two catchments.

The maximum apparent concentrations of FAM in Storm 2 were 12 QSU in the coniferous catchment and 15 QSU in the deciduous catchment, whereas they were 8.6 QSU and 8.7 QSU in Storm 1, respectively. Because the maximum stream discharge in Storm 2 was similar in both catchments, the apparent flux of FAM in the coniferous catchment was lower than that in the deciduous catchment.

The proportion of NIF relative to total elements during the rainstorms (refer to Table 1b and 1c) ranged, in the coniferous catchment, from 5.9% to 41.8% in Storm 1 and from 1.9% to 72.4% in Storm 2. Contrastively, that in the deciduous catchment ranged from 23.4% to 49.6% in Storm 1 and 24.5% to 60.5% in Storm 2. The mean proportions of NIF in the coniferous catchment were 10.2% to 26.3% lower in Storm 1 and 12.2% to 19.1% lower in Storm 2 than those in the deciduous catchment, with a significant difference under all $p < 0.0001$, $n = 22$ (Storm 1), $n = 29$ (Storm 2), also similar to the results during no rainfall periods (Table 1a).

The changes in chemical concentrations of major ions in stream water during the

rainstorms (piper trilinear diagrams; Piper, 1944) are shown in Fig. 8. On the basis of the combination of the rate of free ions expressed in Fig. 8, the flow modes contributing stream water are categorized as following 4 types:

I : $CaSO_4$-$CaCl_2$ type (non-carbonate hardness) originated from surface flow to soil water

II: $Ca(HCO_3)_2$ type (carbonate hardness) originated from soil water to shallow groundwater

III: $NaHCO_3$ type (carbonate alkali) originated from stagnated deep groundwater

VI: $NaSO_4$-NaCl type (non-carbonate alkali) originated from sea water or hot spring

In the coniferous catchment, soil water and shallow ground water (Type I to II) seems to have been the main component of stream water during both rainstorms. However, the combination of major ions in Storm 2 (Fig. 8b left) changed discontinuously from the boundary of Type I and II to the edge of Type I during the rising limb of the hydrograph. In contrast, in the deciduous catchment, the combination distributed between the middle of Type I and Type II in both rainstorms and did not change discontinuously as indicated in the coniferous catchment.

5. Discussion

5.1. Mode of non-free ionic fraction in stream water

We hardly detected K^+ in the stream water of either catchment not only during no rainfall periods but also rainstorms, although it was detected in the shallow soil, indicating that K^+ moved scarcely from the soil to the streams, possibly because most K^+ was absorbed directly from the soils by the trees and other plants or was

irreversibly adsorbed by such clay minerals as vermiculite. Thus K is excludable from the following discussion on the mode of NIF.

NIF-Na, -Mg, and -Ca in natural water can be classified into five chemical forms, which are listed in Table 2. Representative candidate free polyatomic ions in the aquatic environment are MgF^+, $NaSO_4^-$, and $MgPO_4^-$, but these ions are mainly found in seawater (Howard, 1998); these free polyatomic ions mainly dissociate in fresh water or are absent in soils so that the Na and Mg occur as free ions in fresh water streams.

Except for calcium phosphate which is insoluble in fresh water (Guardado *et al.*, 2007), the lowest fresh water solubility among inorganic compounds (hydrate, sulfate, carbonate, nitrate, and phosphate) of Na, Mg, and Ca, at 20 °C and pH 7.0, is that of $NaHCO_3$ (1.04 mol L^{-1}), $Mg(OH)_2$ (1.65×10^{-4} mol L^{-1}), and $CaCO_3$ (1.50×10^{-4} mol L^{-1}). Therefore, in fresh water, the lowest saturated concentrations of Na^+, Mg^{2+}, and Ca^{2+} derived from the dissolution of $NaHCO_3$, $Mg(OH)_2$, and $CaCO_3$ are calculated as about 23.9 g L^{-1}, 4.0 mg L^{-1}, and 6.0 mg L^{-1}, respectively. These calculated values, except for Ca^{2+} in the coniferous catchment from April to June 2007 (7.5 mg L^{-1} at most in Fig. 5), were enough higher (i.e., unsaturated in free ions) than the maximum concentrations measured in the stream water. Moreover, the actual concentrations of Na^+, Mg^{2+}, and Ca^{2+} in the stream water at pH 6.0 to 8.0 could be lower than those measured by ion-analyzer using an eluant with pH 3.0. Thus, the stream water were hardly saturated by Na^+, Mg^{2+}, and Ca^{2+}, and Na, Mg, and Ca derived from the compounds (hydrate, sulfate, carbonate, nitrate, and phosphate) ought to occur mostly as free ions in stream water with pH from 6.0 to 8.0. In addition, cations do not adsorb

onto Al- or Fe-hydroxides in freshwater environments with pH < 8.0, such as the pH of the stream water in these headwater catchments, because they are electropositive ($AlOH_2^+$ or $FeOH_2^+$).

Thus, in our study, except for calcium phosphate, the occurrence of NIF-Na, -Mg, and -Ca in hydration and inorganic compounds scarcely needs consideration. Most NIF-Na, -Mg, and -Ca, therefore, were probably bonded to organic materials or nano-scale phyllosilicates such as clay minerals (e.g., Takahashi *et al.*, 1999). That is, exploring the bonding of these materials is likely to be key to elucidate the transport of Na, Mg, and Ca in the stream water of these headwater catchments.

5.2. NIF dynamics in stream water

5.2.1. Relationship between stream discharge, Si, and NIF during no rainfall periods

In contrast to the inverse relationship observed between stream discharge and the Si concentration during Storm 2 (i.e., dilution of Si by quick-flow component with a low concentration of Si; Fig. 7), the Si concentration during no rainfall periods (Fig. 5) increased as the stream discharge (i.e., baseflow in this case) increased. This result suggests that changes in the Si production are strongly controlled by the baseflow component of stream water.

The correlation coefficients (r) and slopes of the relationships between stream discharge and the Si flux and between the fluxes of Si and NIF during no rainfall periods are shown in Table 3. In the correlation equations, the y-intercept was set to zero, because discharge of Si does not occur without stream discharge, and no NIF production occurs without stream discharge (i.e., without discharge of Si). Against the

wash load flux as mentioned in Section *3.5.* (i.e., not always necessarily represent good correlations), the relationships are expressed as follows under the good correlation (r = 0.99, $p < 0.0001$, n = 54) and the different coefficient "a":

$$Si_{(baseflow)} = a\, Q_{(baseflow)}, \quad (3)$$

where $Si_{(baseflow)}$ is the Si flux in the stream water during the no rainfall periods, the coefficient a represents the average Si concentration, and $Q_{(baseflow)}$ is the stream discharge during no rainfall periods (i.e. baseflow). When the stream water was collected (and thus the Si concentration was measured), the maximum stream discharge was 3.19 L s^{-1} ha^{-1} and 5.06 L s^{-1} ha^{-1} in the coniferous and deciduous catchments, respectively. Thus, in the strict sense, when we calculate the baseflow component of the stream water during the rainstorms ($Q_{(baseflow\ in\ rainstorm)}$ in Eqs. 1, 5, and 6, Eq 3 is available to the baseflow component below 3.19 L s^{-1} ha^{-1} and 5.06 L s^{-1} ha^{-1} in the coniferous and deciduous catchments, respectively.

In contrast, the correlations between the fluxes of Si and NIF in the stream water during the no rainfall periods were also high ($r > 0.92$, $p < 0.0001$, n = 30) in both catchments (Table 3). The NIF flux during no rainfall periods ($NIF_{(baseflow)}$) can therefore be expressed by $Si_{(baseflow)}$ and Eq. 3 as follows:

$$NIF_{(baseflow)} = b\, Si_{(baseflow)} = ab\, Q_{(baseflow)}. \quad (4)$$

Eq 4 indicates that the ratio of the NIF discharge to the Si discharge in stream water was approximately constant during the no rainfall periods. The values of the coefficient b are shown in Table 3. Even though Si is naturally included in nano-scale phyllosilicates, the relationship between Si and NIF expressed by Eq. 4 does not necessarily explain the transport form of the major metals bonded to nano-scale

phyllosilicates (e.g., substitution in lattices, invasion into the interlayer spaces, or ion adsorption on the surfaces) because of occurring simple silicic acid ions. However, the high correlation between Si and NIF during the no rainfall periods may have some implications regarding the transport of Si and NIF, because during the rainstorms the Si flux (Table 4) did not usually correlate strongly (i.e., $r < 0.80$) with NIF fluxes. In particular, during Storm 1 (Table 4a), the correlations tended to be weak except for NIF-Mg in the coniferous catchment, even when the baseflow component accounted for most of the stream water (94% and 97% in the coniferous catchment and deciduous catchment, respectively; Hirano *et al*., 2009).

5.2.2. Relationship between stream discharge, Si, and NIF during rainstorms

The correlation coefficients (r) and slopes of the relationships between stream discharge and the Si flux and between the fluxes of Si and NIF during rainstorms are shown in Table 4.

The concentrations of Si in both catchments during the rainstorm decreased slightly (a few mg L^{-1}) with an increase in stream discharge, indicating that the Si, originated in the baseflow component in stream water, could have been diluted with the quick-flow component containing the low Si concentration. This finding was consistent with those from no rainfall periods, that is, more baseflow equates to higher Si concentration.

In both rainstorms, as well as the cases during the no rainfalls, the Si flux correlated strongly ($r \geq 0.80$, $p < 0.0001$, $n = 24$ and 29 for the coniferous catchment and deciduous catchment, respectively) with the stream discharge in both catchments. The values of the coefficient a, however, were smaller in both catchments than its

value during the no rainfall periods (i.e., $a_{(\text{baseflow})} > a_{(\text{Storm 1})} > a_{(\text{Storm 2})}$). Therefore, compared with the no rainfall periods, the rate of increase in the Si flux relative to that in the stream water was lower during rainstorms, probably because the low Si concentration of the quick-flow component of the stream water caused the Si concentration in the total stream water to be relatively low. This finding suggests that, as indicated in Section *5.2.1*, the Si production during rainstorms is also strongly controlled by Si in the baseflow component of the stream water.

The weak correlations ($r < 0.60$) between the fluxes of Si and NIF in some cases in Table 4 suggest that, in contrast to no rainfall periods (Table 3), NIF was not necessarily increased according to the increase in Si during rainstorms. Though the ratio of NIF to Si reflects in part the different values of the *b* coefficient (Tables 3 and 4), the low correlations ($r < 0.60$, Table 4) may reflect either an increased or reduced transport of NIF by the quick-flow component of the stream water in those cases. Thus, in analyses of NIF transport during rainstorms, NIF should be classified according to whether it derives from the baseflow or the quick-flow component of the stream water. In contrast, as shown in the deciduous catchment in Table 4b, strong correlations ($r \geq 0.80$) may reveal that the flow components of the stream water did not implicate the result in an increase in transport of Si and NIF.

5.3. Bonding possibility of Na, Mg, and Ca to FAM

5.3.1. Origin of FAM and NIF during rainstorms

Water extractable FAM tended to be stored in the shallower part of soil in the coniferous catchment than in the deciduous catchment (Fig. 4 and Section *4.1.*). In

contrast, soil porosity and saturation hydraulic conductivity are similar in both catchments (Section *2.2.*). These findings may imply that the hydrological process, such as near-surface flow represented by biomatflow caused dominantly in the coniferous catchment, may have controlled the downward movement of FAM.

In Storm 1, the apparent fluxes of FAM were mostly $\leq$ 2.0 QSU L s^{-1} ha^{-1} in both catchments, and the maximum fluxes were 4.9 QSU L s^{-1} ha^{-1} and 6.4 QSU L s^{-1} ha^{-1} in the coniferous and deciduous catchments, respectively. In contrast, in Storm 2, the apparent fluxes were $\geq$ 2.0 QSU L s^{-1} ha^{-1} in both catchments, and the maximum fluxes were 53.3 QSU L s^{-1} ha^{-1} and 113.6 QSU L s^{-1} ha^{-1} in the coniferous and deciduous catchments, respectively. Thus, the production of FAM was relatively small during Storm 1, which was a small rainstorm that contributed only a small quick-flow component to the total stream water (6% and 3% in the coniferous and deciduous catchments, respectively; Hirano *et al*., 2009) and consequently produced smaller changes in the stream hydrograph than Storm 2. Thus, during rainstorms, most FAM likely originated at relatively shallow depth in the soil as shown in Fig. 4a.

During the heavy rainstorm, both surface or near-surface water (i.e., quick-flow component) and deep soil water was dominant in the coniferous catchment, whereas both shallow and deep soil water was dominant in the deciduous catchment (Fig. 8). Thus NIF and FAM production could be strongly controlled by the main flow component of stream water, which was different between the coniferous and deciduous catchment. Accordingly, when we analyze the relationship between FAM and NIF during rainstorms, we should take into account whether the NIF in the stream water derived primarily from the baseflow (deep soil) or quick-flow (near-surface or shallow

soil).

As indicated in Section *5.2.2*, the Si production in the stream water during the rainstorms seems to have been controlled mainly by Si included in the baseflow component of the stream water (e.g., $a_{(\text{baseflow})} > a_{(\text{Storm 1})} > a_{(\text{Storm 2})}$ in Tables 3 and 4). In addition, the maximum stream discharge during the no rainfall periods (i.e., maximum baseflow) were 3.19 L s^{-1} ha^{-1} and 5.06 L s^{-1} ha^{-1} in the coniferous and deciduous catchments, respectively; corresponding to 0.6 and 1.3 times the maximum baseflow component calculated for Storm 2 using Eq. 1. In other words, specifically in the coniferous catchment, the maximum baseflow component during Storm 2 was more than the baseflow during the no rainfall periods.

Accordingly, if we could extrapolate Eq. 4 for calculating the baseflow component in the coniferous catchment during Storm 2, we can modify Eq. 4 for the two catchments to express NIF originating from the baseflow component during the rainstorms as follows:

$$NIF_{(\text{baseflow in rainstorm})} = b\,Si_{(\text{baseflow in rainstorm})} = ab\,Q_{(\text{baseflow in rainstorm})}, \quad (5)$$

where $Si_{(\text{baseflow in rainstorm})}$ is the Si flux originating from the baseflow component of the stream water during rainstorms. By combining Eqs. 1, 2, and 5, we obtain:

$$\Delta NIF = NIF_{(\text{rainstorm})} - ab\,Q_{(\text{baseflow in rainstorm})}$$

$$= NIF_{(\text{rainstorm})} - ab\;Q_{(\text{rainstorm})}\left(1 - Q_{(\text{quick-flow})} / Q_{(\text{rainstorm})}\right). \quad (6)$$

Eq. 6 can thus be used to examine the relationship between NIF and FAM transported in the stream water during rainstorms, which is mainly contained in the quick-flow component passed through relatively shallow soil with a high FAM content (Fig. 4a).

5.3.2. Relationship between FAM, NIF, and ΔNIF during the rainstorms

The relationships between the fluxes of FAM, Si, NIF, and ΔNIF in the stream water during rainstorms are shown in Table 5. In these correlations, the y-intercept (*d*) is a non-zero value because NIF can be transported in the stream water during the no rainfall periods, when the FAM flux is very small. In the case of Storm 1, we could not determine whether the samples were collected on the rising or falling limb of the hydrograph because the small rainfall amount produced only small changes in the hydrograph, but in the case of Storm 2, we classified the samples according to when they were collected. Thus, for the relatively weak correlations during Storm 2 ($r <$ 0.70), we also calculated correlations for samples collected during the rising and falling limbs of the hydrograph separately, and we show respectively those correlation coefficients in parentheses in Table 5.

For Storm 1 (Table 5a), when the quick-flow component accounted for ≤ 6% of the stream water (Hirano *et al.*, 2009), we were unable to calculate correlation coefficients for the FAM–ΔNIF-Ca relationship in the deciduous catchment, because ΔNIF-Ca, calculated with Eq. 6, was generally 0 mg s^{-1}. Except for FAM versus ΔNIF-Na in the deciduous catchment (r = 0.86, p = 0.0009, n = 16), the correlations between FAM and Si, NIF, and ΔNIF were low ($r \leq 0.60$, n = 22 for the coniferous catchment and n = 16 for the deciduous catchment). Thus, these low correlations likely reflect the effect of the high proportion of baseflow component (≥ 94% of the stream discharge; Hirano *et al.*, 2009) on the variation of FAM, derived mostly from the shallow soil by the quick-flow component. These findings indicate that the transport of NIF (or ΔNIF), that is, the bonding of Na, Mg, and Ca to FAM, hardly differed during

the small rainstorm from that during the no rainfall periods because of the relatively small change in the quick-flow component of the stream water.

Takahashi *et al*. (1999) mentioned that the inorganic particles coated by humic material (organic-inorganic complex) should have been regarded as important particulate matter which shows different affinities to various ions from inorganic particulates without the organic coating. In addition, they indicated that the colloidal inorganic particles coated with humic substances were expected to be significantly important in the environment. Thus, as well as the case during the no rainfalls, Na, Mg, and Ca may have been bonded not only to FAM (Choppin and Shanbhag, 1981; Livens, 1991) but also to nano-scale phyllosilicates, organic acids of which the concentration was implicitly indicated by our measurement in the ion-analyzer and the 3d-EEM, other unknown materials such as citric, tartaric, lactic, and malic acids (Stevenson, 1994), or to else which is soluble in freshwater (Guardado *et al.*, 2007).

In Storm 2 (Table 5b), when the quick-flow component accounted for ≥ 30% of the stream discharge (Hirano *et al.*, 2009), the correlations between FAM and ΔNIF were strong ($r \geq 0.81$, $p < 0.0001$, $n = 22$) in the coniferous catchment. This result supports the interpretation that the quick-flow component during the large rainstorm in the coniferous catchment, as shown at the edge of Type I in Fig. 8, may have transported FAM and ΔNIF together from the relatively shallow soil layer. In contrast, in the deciduous catchment, the strong correlations ($r \geq 0.83$, $p < 0.0001$, $n = 26$) of FAM with both NIF and ΔNIF may have resulted from their derivation from soil water and shallow groundwater (Fig. 8) that passed through the shallow to deep part of soil containing higher FAM concentrations than those in the coniferous catchment (Fig.

4a).

Furthermore, FAM was also correlated more strongly with Si in the deciduous catchment (r = 0.87, p < 0.0001, n = 26) than in the coniferous catchment (r = 0.73, p < 0.0001, n = 26). Together with the strong correlations between Si and NIF in the deciduous catchment during Storm 2 (Table 4b), these findings may indicate the interpretation that during heavy storms, Na, Mg, and Ca bond more likely to FAM and also possibly to nano-scale phyllosilicates (organic–inorganic interactions as indicated by Takahashi *et al.*, 1999) in the headwater stream of the deciduous catchment, compared with the coniferous catchment. This thing may result from the interaction between rainwater pathways in relatively deep part of soil compared to the near-surface and FAM percolated into the deeper part of soil in the deciduous catchment than in the coniferous catchment.

5.4. Effect of environmental factors on NIF production

Using a chemical model, Mantoura *et al*. (1978) showed that, in freshwater lakes, compounds of Mg and Ca with sulfate (-SO_4) and carbonate (-CO_3) accounted for ≤ 1% of their total concentrations, and it has since been assumed that most Na, Mg, and Ca occurs as free ions in natural freshwater bodies. However, in our study (Figs. 5, 7, and Table 1), NIF-Na, -Mg, and -Ca in stream water sometimes accounted for half or more of the total concentrations of these elements. This was predominant in the deciduous catchment, suggesting that NIF are not a negligible feature in freshwater streams when the species of Na, Mg, and Ca are considered. Although the baseflow pH was about 1.0 pH unit higher in the coniferous catchment than in the deciduous

catchment, the concentrations of free ions in the coniferous catchment were 1 to 4 mg L^{-1} higher than those in the deciduous catchment. In other words, increased production of free ions due to the lower stream water pH never provides the lower concentrations of free ions in the deciduous catchment (i.e., the higher proportion of NIF). In addition, the flux of Na^{+}, Mg^{2+}, and Ca^{2+} to the forests were approximately the same in both catchments (Section *3.2.*). Therefore, the proportion of NIF must indicate that the bonding of Na, Mg, and Ca between the soils and streams may account for the high percentage of NIF in the stream water.

No human activities, such as thinning to reduce tree density or fertilizing, took place in either catchment during the observation period. Furthermore, geographical, topographical, geological, and climatic conditions were almost the same in both catchments. Consequently, the differences in chemistry of Na, Mg, and Ca in the stream water between the two catchments; specifically both in the higher free ion concentration in the coniferous catchment than in the deciduous catchment (Fig. 6) and in the proportion of NIF which was from 10% to 26% lower on average in the coniferous catchment than in the deciduous catchment (Table 1); may primarily reflect the effects of the different vegetation on the bonding of Na, Mg, and Ca.

In particular, Fig. 8 also emphasizes that the main flow pathways contributing to stream water during Storm 2 could have been different in the coniferous and deciduous catchments. The stream water (and thus FAM) in the coniferous catchment during Storm 2 was likely originated in near-surface water and shallow groundwater, whereas it was likely originated in soil water to shallow groundwater in the deciduous catchment. The unique flow generation (biomatflow) from near-surface at the slope

during rainstorms in the coniferous catchment could be one of the causes to transport much FAM to stream water and consequently to store little FAM in the deep part of soil (Fig. 4a).

6. Conclusions

We investigated the transport of major metals by measuring the concentrations of Na, Mg, Ca, Si, and fulvic acid-like materials in two mountainous headwater streams in Japan, one surrounded by coniferous and the other by deciduous forest. The conclusions are not necessarily being generalized because only data sets for two rainstorms and two headwater catchments were prepared in the presented study. However, together with the data during no rainstorms, the following outlines can be mentioned for the transport and bonding possibility of major metals caused in the headwater streams by differing vegetation:

(1) The proportion of non-free ionic fractions to total metal elements ranged from 0% up to 70% in two streams during both no rainfall period sand rainstorms and was lower in the coniferous catchment than in the deciduous catchment, though most Na, Mg, and Ca has previously been assumed as free ions in natural freshwater environments.

(2) In the stream water during no rainfall periods, as well as during small rainstorms, some non-free ionic fractions in two streams were probably transported in bonding to unknown materials including nano-scale phyllosilicates (clay minerals), organic acids, or else.

(3) During heavy rainstorms, non-free ionic fractions in two streams could have mostly

been in bonding to humic substances and possibly to nano-scale phyllosilicates; which was dominantly enhanced in the deciduous catchment. This finding could have been due to the difference in flow pathways contributing to stream water: both surface or near-surface water (i.e., overland flow or biomatflow,) and shallow groundwater was dominant in the coniferous catchment, whereas both soil water (i.e., subsurface flow) and shallow groundwater was dominant in the deciduous catchment.

(4) Above findings imply that the environmental controls, such as implication among the differences in rainstorm size (i.e., weather condition), the distribution and content of humic substances in soils (i.e., vegetational condition), and the resultant rainwater flow pathways contributing to stream water (i.e., hydrological condition), provided the variable organic-inorganic interactions in the headwater streams where geographical, topographic, geological, and climatic conditions are similar.

Headwaters are the most elementary topographic unit to examine catchment hydrology. Consequently, the data on bonding of major metals, linked with the effect of environmental controls in headwater streams, should be fundamental and useful to understand the chemical species of major metals in the complicated and confusing nature as stream catchments. It is hoped that the accumulation of data sets based on field observations will improve the understanding of chemical species of major metals which was believed to occur mostly as free ions in freshwater environments.

Acknowledgement

We thank the Rijin-kai Association, the owner of the Nariki catchment, for permission to use the catchments for our observations. The present study was partially

funded by a grant for environmental research from the Sumitomo Foundation, Japan (No. 083295).

References

Artinger, R., Bukau, G., Geyer, S., Fritz, P., Wolf, M., Kim, J.I., 2000. Characterization of groundwater humic substances: Influence of sedimentary organic carbon. Appl. Geochem. 15, 97-116.

Choppin, G.R., Shanbhag, P.M., 1981. Binding of calcium by humic acid. J. Inorg. Nucl. Chem. 43, 921-922.

Coble, P., Schultz, C., Mopper, K., 1993. Fluorescence contouring analysis of DOC intercalibration experiment samples: a comparison of techniques. Mar. Chem. 41, 173–178.

Coble, P., 1996. Characterization of marine and terrestrial DOM in seawater using excitation-emission matrix spectroscopy. Mar. Chem. 51, 325-346.

Coble, P., Del Castillo, C., Avril, B., 1998. Distribution and optical properties of CDOM in the Arabian Sea during the 1995 SW monsoon. Deep-Sea Res. II 45, 2195–2223.

Fellman, J.B., Hood, E., Robert G. M. Spencer, R.G.M., 2010. Fluorescence spectroscopy opens new windows into dissolved organic matter dynamics in freshwater ecosystems: A review. Limnol. Oceanogr. 55, 2452–2462.

Guardado, I., Urrutia, O., Garcia-Mina, J.M., 2007. Size distribution, complexing capacity, and stability of phosphate-metal-humic complexes. J. Agric. Food Chem. 55, 408-413.

Hirano, T., Terajima, T., Nakamura, T., Aoki, F., Sakai, M., 2008. Surface and near-surface runoff at slopes of the unmanaged coniferous forests and the natural deciduous forests in Nariki nested catchment. Trans. Jpn. Geomorph. Union. 29, 255-280 (in Japanese with English abstract and captions).

Hirano,T., Terajima, T., Nakamura, T., Sakai, M., Aoki, F., Nanami, A., 2009. The differences in the short-term runoff characteristics between the coniferous catchment and the deciduous catchment, the effect of storm size on stormflow generation processes of small forested catchments. J. Jpn. Soc. Hydrol. Water Resour. 22, 24-39 (in Japanese with English abstract and captions).

Howard, A.G., 1998. Aquatic environmental chemistry, Oxford chemistry primers: 57, p90, Oxford University Press.

Inosato, H., Kanno, S., Shindo, S., Watanabe, K., 1980. Local geology in Japan, Kanto region. Asakura Publ. Co. Ltd., Tokyo (in Japanese).

Lakowicz, J.R., 1999. Principles of fluorescence spectroscopy, 2nd ed. Springer.

Livens, F.R., 1991. Chemical reactions of metals with humic material. Environ. Pollution 70, 183-208.

Majzik, A., Tombacz, E., 2007. Interaction between humic acid and montmorillonite in the presence of calcium ions I. Interfacial and aqueous phase equilibria: adsorption and complexation. Organic Geochem. 38, 1319-1329.

Malcolm, R.L., 1990. Humic substances in soil and crop sciences: Selected readings (eds. P. MacCarthy *et al.*), ASAI & SSSA, Madison. p13-35.

Mantoura, R.F.C., Dickson, A., Riley, J.P., 1978. The complexation of metals with humic materials in natural waters. Estuarine Coastal Mar. Sci. 6, 387–408.

McDowell W.H., 2003. Dissolved organic matter in soils—future directions and unanswered questions. Geoderma 113, 179-186.

Mostofa, K., Honda, Y., Sakugawa, H., 2005. Dynamics and optical nature of fluorescent dissolved organic matter in river waters in Hiroshima Prefecture, Japan. Geochem. J. 39, 257–271.

Nogi, T., 2007. Temporal and spatial changes in rainfall amount and chemistry in an unmanaged evergreen coniferous forest and natural deciduous broaleaf forest. Graduation thesis of Chiba University, 29pp., in Japanese (unpublished).

Piper, A.M., 1944. A graphic procedure in the geochemical interpretation of water-analyses. Trans. Am. Geophys. Union 25, 914-928.

Romkens, P.F., Bril, J., Salomons, W., 1996. Interaction between Ca2+ and dissolved organic carbon: implication for metal mobilization. Applied Geochem.11, 109-115.

Sidle, R.C., Hirano, T., Gomi, T., Terajima, T., 2007. Hortonian overland flow from Japanese forest plantations – an aberration, the real thing, or something in between ?. Hydrol. Process. 21, 3237-3247.

Stevenson, F.J. 1994. Humus Chemistry. 2nd ed., 497pp., Wiley. New York.

Strellis, D.A., Hwang, H.H., Anderson,T.F., Landsberger,S. 1996. A comparative study of IC, ICP-AES, and NAA measurements on chlorine, bromine, and sodium in natural waters. J. Radioanal. Nur. Chem. 211, 473-484.

Suzuki, Y., Nakaguchi, Y., Hiraki, K., Nagao, S., Kudo, M., Kimura, M., 1998. Characteristics of the fluorescent substances in the Yodo River system by three-dimensional excitation emission matrix spectroscopy. Chikyu Kagaku 32, 21–30.

Takahashi, Y., Minai, Y., Ambe, S., Makide, Y., Ambe, F., 1999. Comparison of adsorption behavior of multiple inorganic ions on kaolinaite and silica in the presence of humic acid using the multi tracer technique. Geochimica et Cosmochimica Acta. 63, 815-836.

Takahashi, Y., Kimura, T., Minai, Y., 2002. Direct observation of Cm (III) – fulvate species on fulvic acid-montmorillonite hybrid by laser-induced fluorescence spectroscopy. Geochimica et Cosmochimica Acta. 66, 1-12.

Terajima, T., Sakamoto, T., Nakai, Y., Kitamura, K., 1997. Suspended sediment discharge in subsurface flow from the head hollow of a small foreated watershed, northern Japan. Earth Sur. Proc. & Landf. 22, 987-1000.

Terajima, T., Moriizumi, M., 2013. Temporal and spatial changes in dissolved organic carbon concentration and fluorescence intensity of fulvic acid like materials in mountainous headwater catchments. J. Hydrol. 479, 1-12.

Thurman, E.M., 1985. Organic geochemistry of natural waters. Martinus Nijhoff/Dr W. Junk Publishers. Dordrecht, 497pp.

Tipping, E. 1993. Modeling ion binding by humic acids. Physicochemical and Engineering Aspects. 73, 117-131.

Tokyo Prefectural Public Work Institute, 2002. Geological map of the Okutama area. Tokyo Prefecture (in Japanese).

Wels, C., Cornett, R.I., Lazerte, B.D., 1991. Hydrograph separation: A comparison of geochemical and isoyopic tracers. J. Hydrol. 122, 253-274.

Wilson, M.A., Tran, N.H., Milev, A.S., Kannangara,G.S.K., Volk,H., Lu, G.Q.M., 2008. Nanomaterials in soils. Geoderma 146, 291-302.

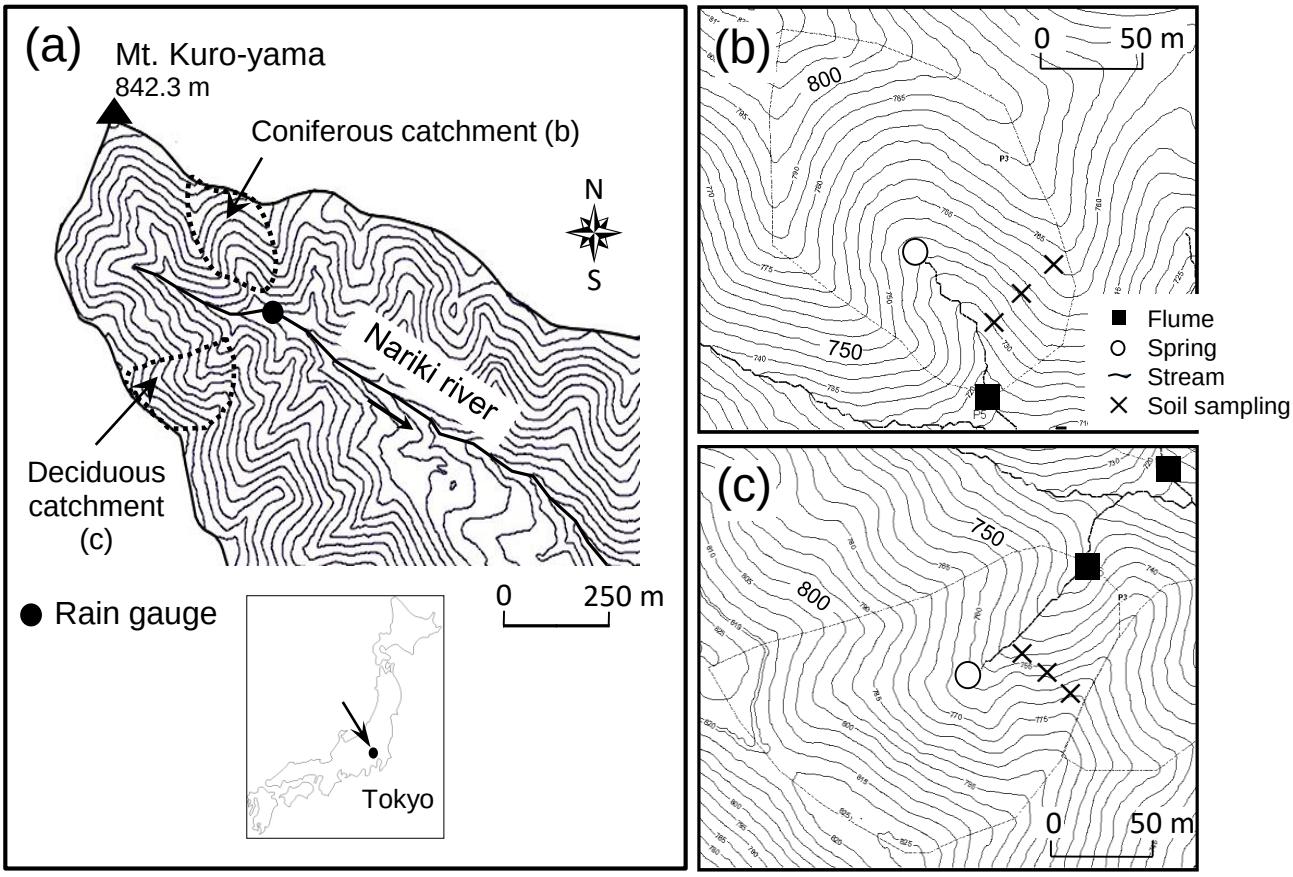

Figure 1. Location and topographic maps of the Nariki catchment and headwater catchments. (a) Nariki catchment, (b) Coniferous catchment, (c) Deciduous catchment. Contour intervals of the Nariki catchment (a) and headwater catchments (b and c) are 10 and 5 m, respectively.

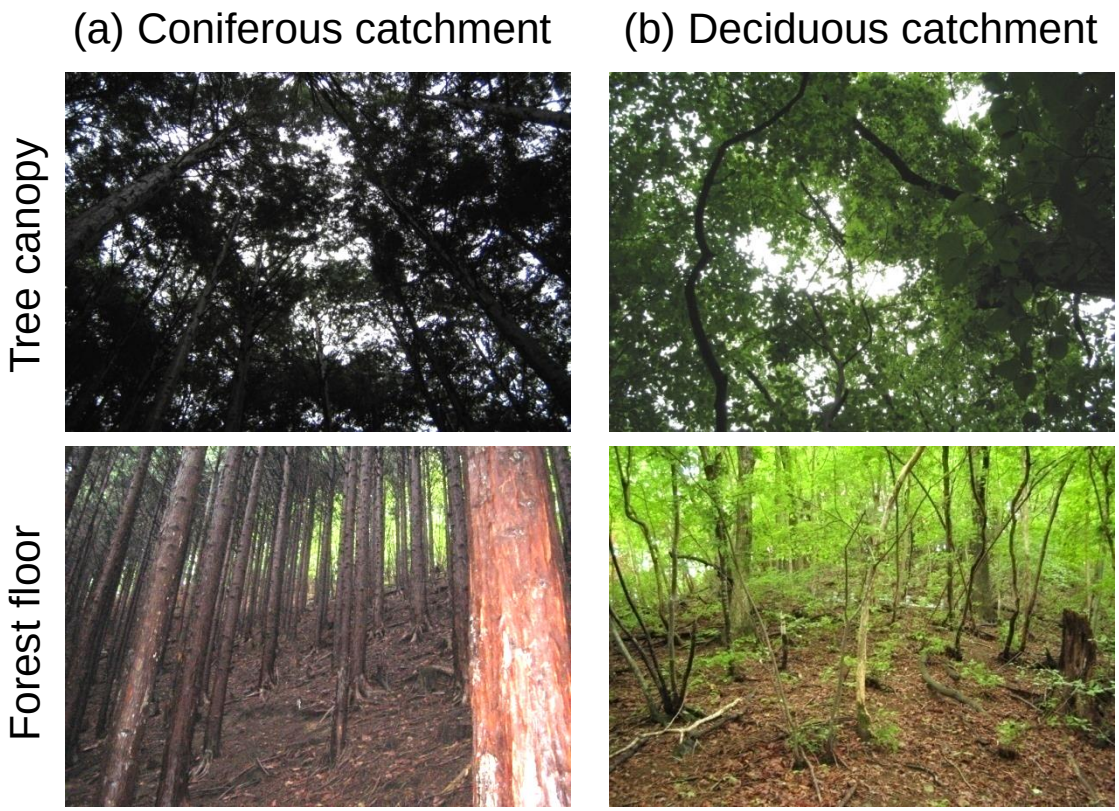

Figure 2. Tree canopies and understory vegetation in the headwater catchments in the summer of 2006.

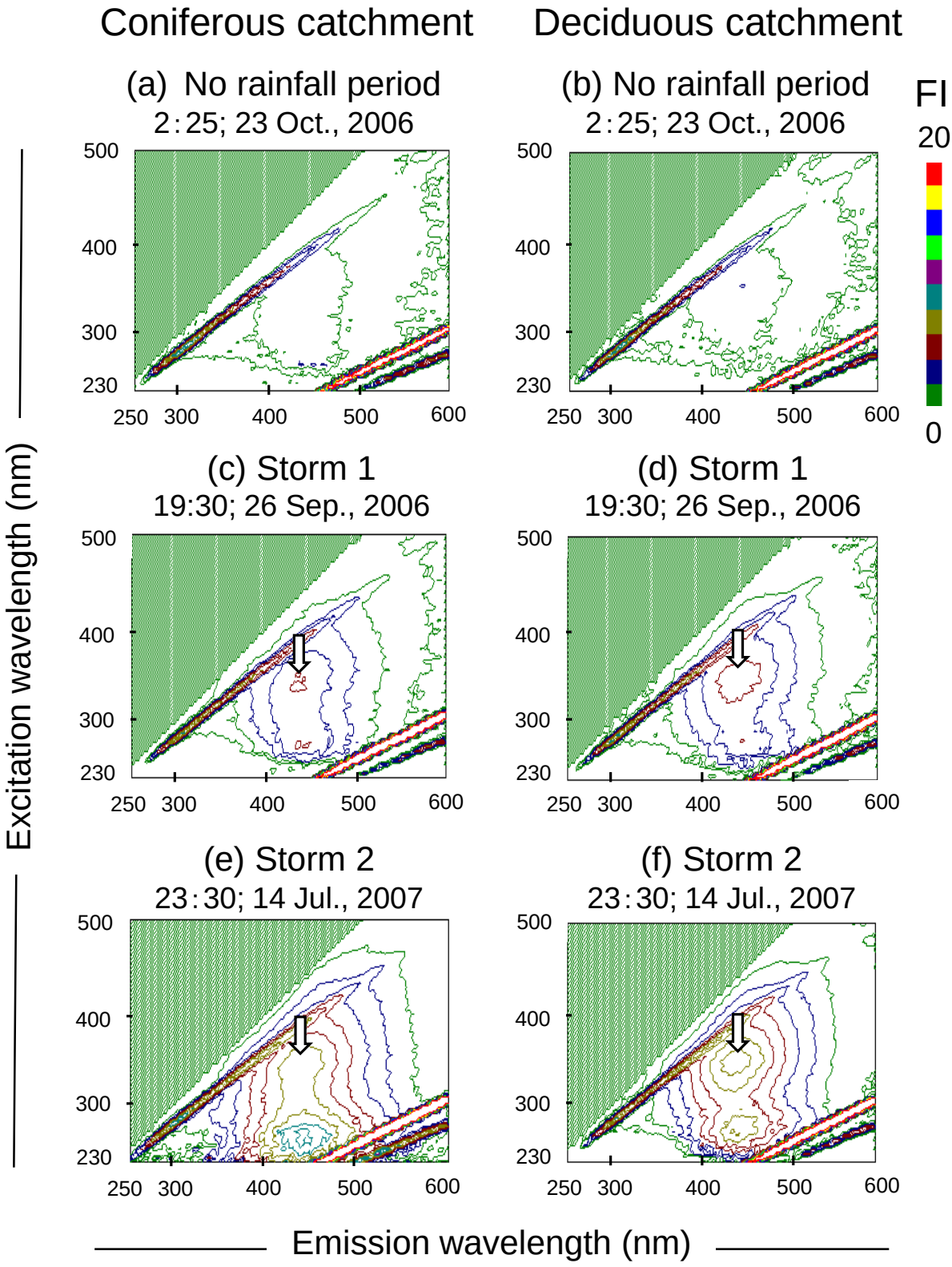

Figure 3 Typical EEM spectra for the different stream flow regimes. The arrows show the visible peaks in fluorescence intensity (FI) at around Ex/Em: 340/440 during the rainstorms. Contour intervals of FI are 1.0.

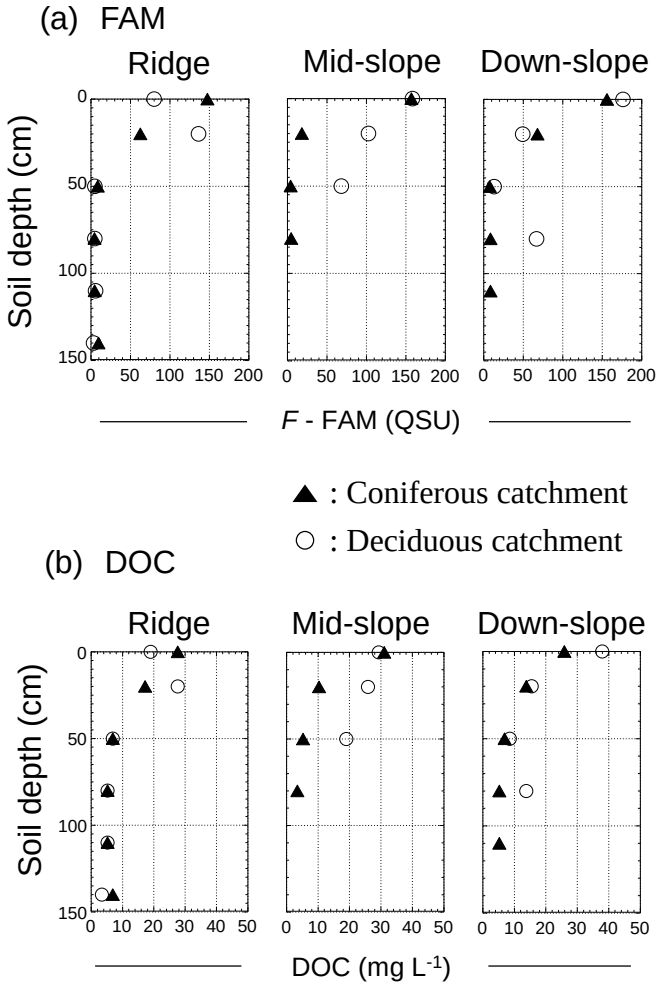

Figure 4. Distribution of water extractable fulvic acid-like materials (FAM) and dissolved organic carbon (DOC) in soils.

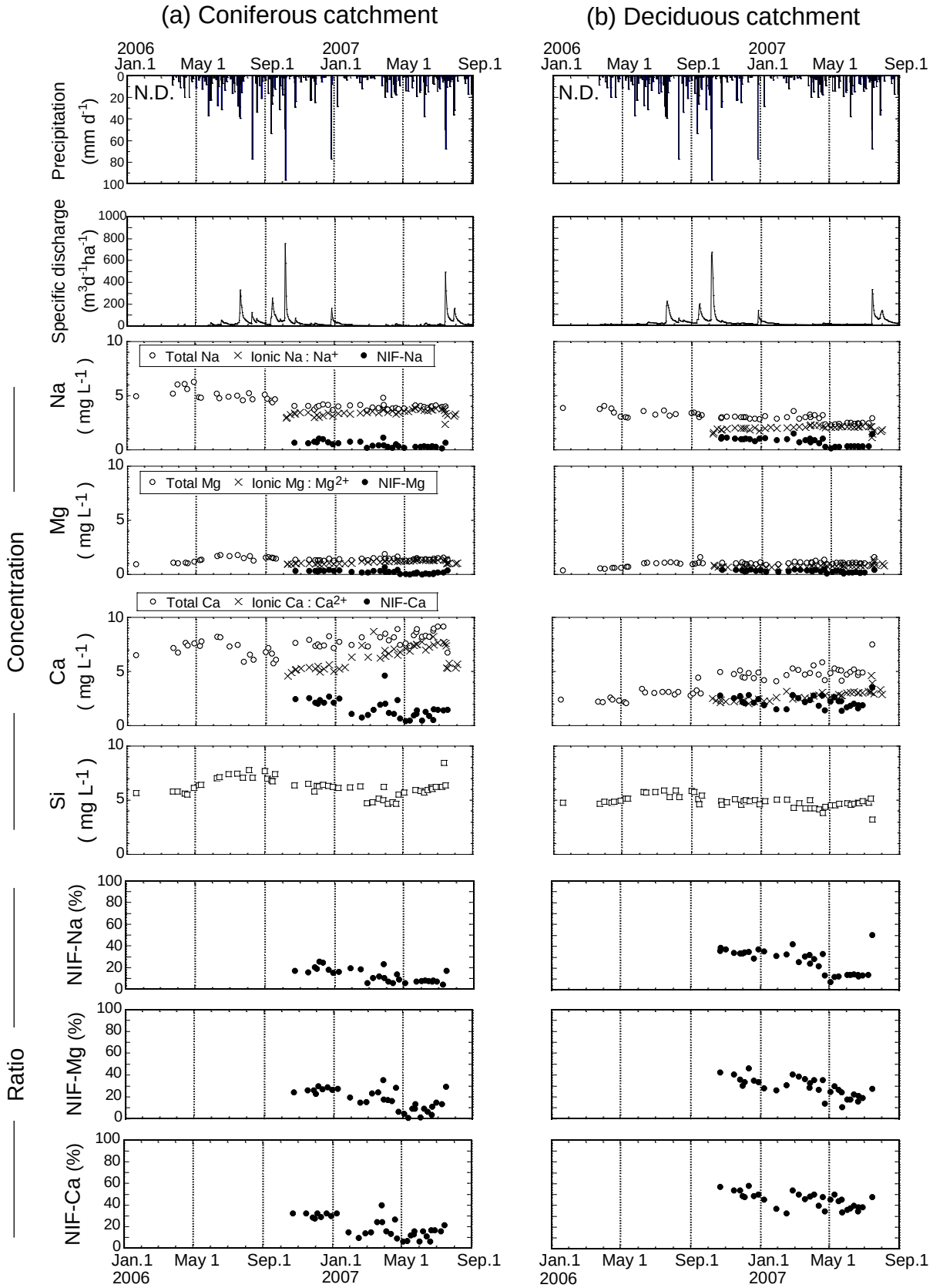

Figure 5. Concentrations of major metals (Na, Mg, and Ca) and silicon (Si), and the proportion of non-free ionic fractions (NIF) relative to total elements in stream water during no rainfall periods from 2006 to 2007. N.D. in the hyetograph shows no data

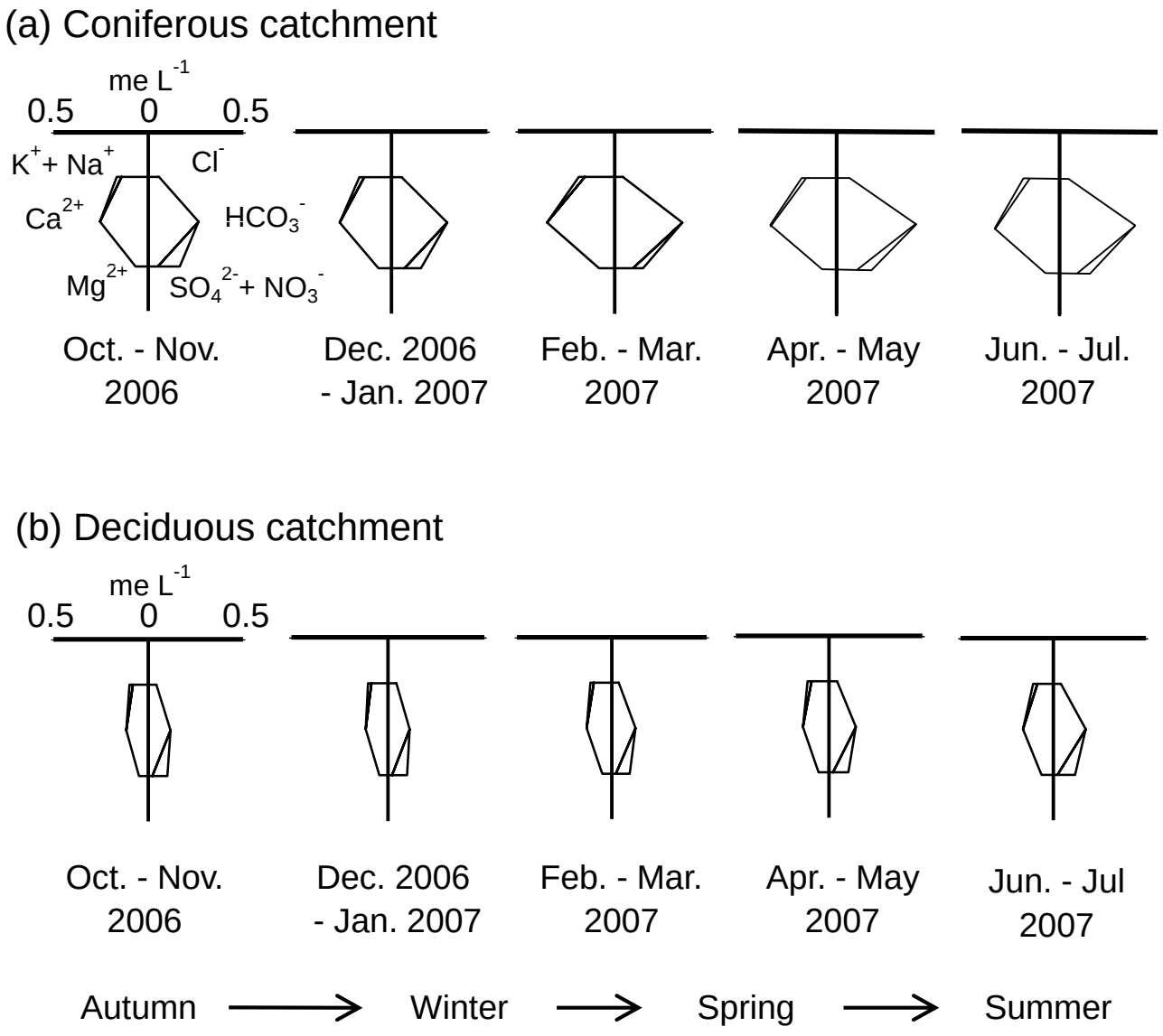

Figure 6. Seasonal changes in major ions in stream water during no rainfall periods, which were derived from the arithmetic mean of the concentration data during two months

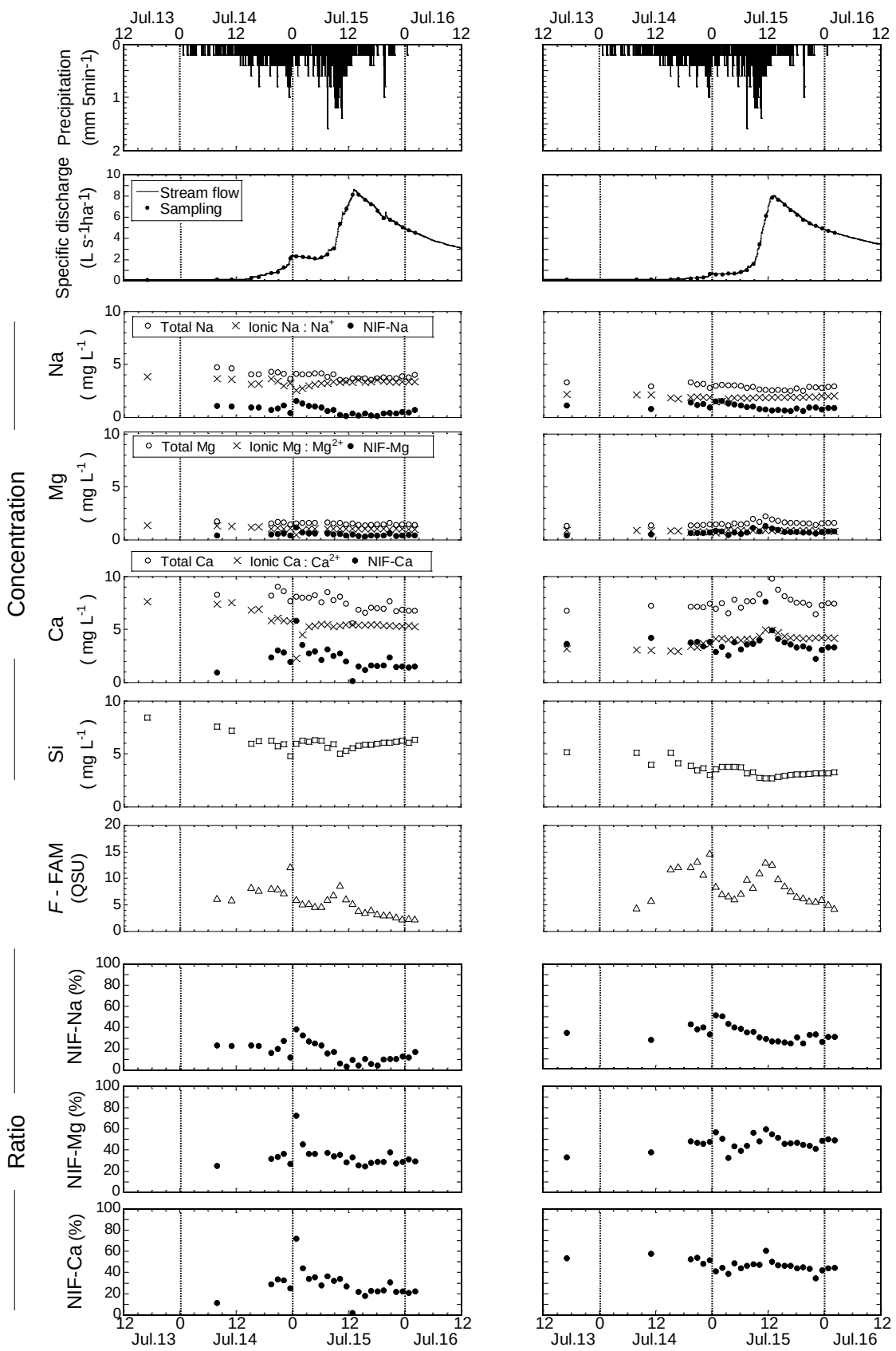

Figure 7. Concentrations of major metals (Na, Mg, and Ca) and silicon (Si), peak fluorescence intensity (*F*-FAM), and the proportion of non-free ionic fractions (NIF) relative to total elements in stream water during a typhoon storm in 2007 (Storm 2).

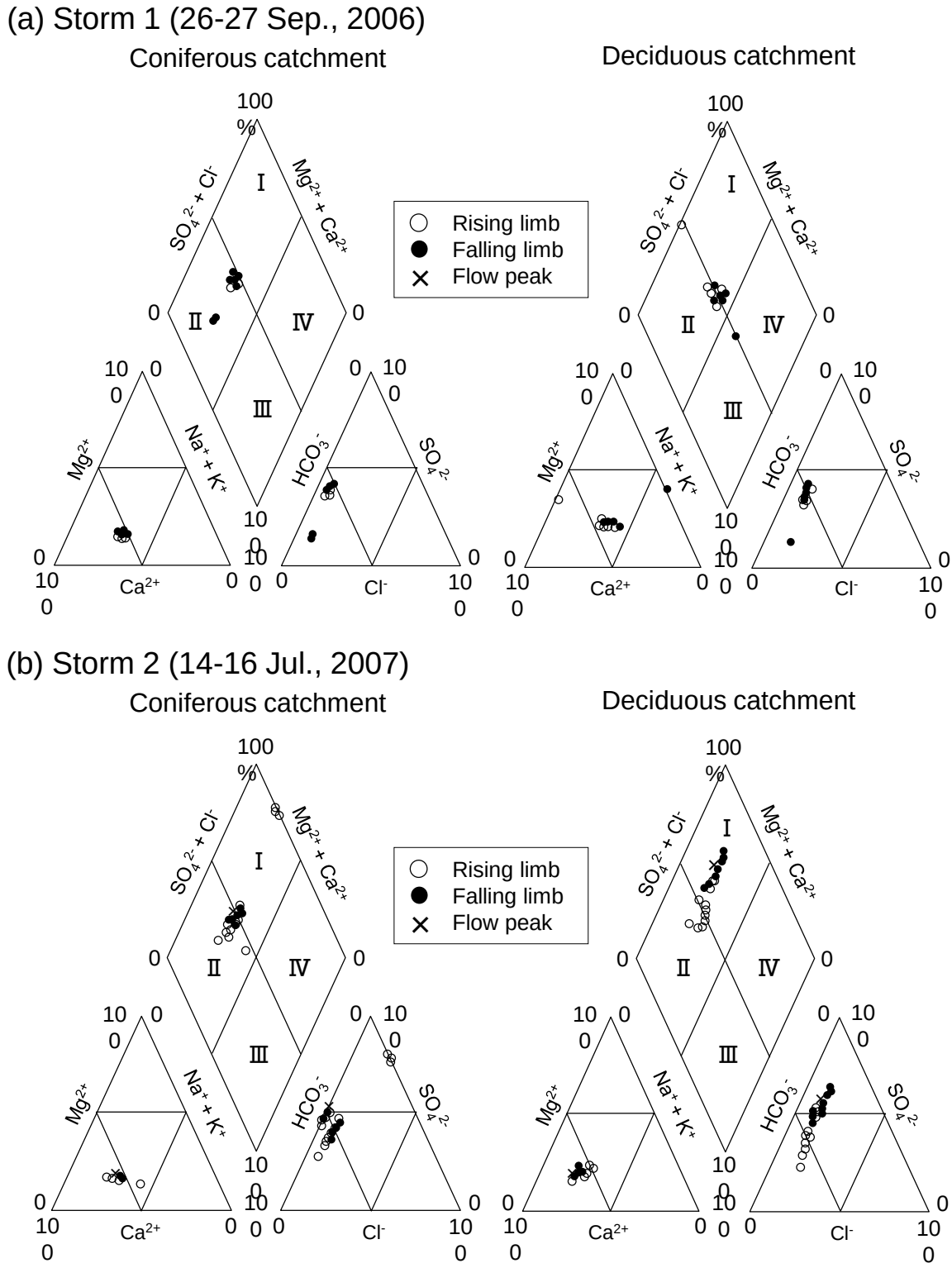

Figure 8. Piper-trilinear diagrams of stream water chemistry (compositional changes in major ions) during the rainstorms.

I：$CaSO_4$-$CaCl_2$ type (non-carbonate hardness) originated from surface flow to soil water.
II：$Ca(HCO_3)_2$ type (carbonate hardness) originated from soil water to shallow groundwater.
III：$NaHCO_3$ type (carbonate alkali) originated from stagnated deep groundwater.
IV：$NaSO_4$-NaCl type (non-carbonate alkali) originated from sea water or hot spring.

Table 1. Proportion of non-free ionic fractions (NIF) relevant to total elements in the stream water (unit : %)

(a) No rainfall periods		Coniferous catchment	Deciduous catchment
NIF-Na	Range	4.4～25.6	7.3～50.3
	Average	13.0	26.6
NIF-Mg	Range	0.6～35.6	10.7～46.3
	Average	17.7	29.0
NIF-Ca	Range	6.2～40.0	32.5～58.0
	Average	19.6	45.0

(b) Storm 1		Coniferous catchment	Deciduous catchments
NIF-Na	Range	16.5～33.5	25.1～43.5
	Average	24.8	35.0
NIF-Mg	Range	25.0～41.8	33.9～48.5
	Average	31.8	42.0
NIF-Ca	Range	5.9～29.1	23.4～49.6
	Average	14.2	40.5

(c) Storm 2		Coniferous catchment	Deciduous catchment
NIF-Na	Range	3.3～38.2	24.5～51.3
	Average	16.4	33.9
NIF-Mg	Range	24.5～72.4	32.6～59.8
	Average	34.6	46.8
NIF-Ca	Range	1.9～72.1	34.3～60.5
	Average	28.0	47.1

Table 2. Non-free ionic forms of sodium (Na), magnesium (Mg), and calcium (Ca), and the possible bonding partner or ligand group in aquatic environment.

Non-free ionic forms of Na, Mg, and Ca	Possible bonding partner or ligand group
◆ Inorganic materials	
Hydration	⇨ H_2O, OH^-
Adsorption / Substitution in phyllosilicates	⇨ Si, Al
Inorganic compounds	⇨ F^-, SO_4^{2-}, CO_3^{2-}, NO_3^-, PO_4^{3-} Al- or Fe- hydroxide, etc
◆ Organic materials	
Adsorption on humic substances	⇨ Carboxyl group : COO^- Phenolic group : Ph-OH Amino group : $-NH_2$ Imino group : -NH
Complex of organic acids	⇨ Oxalate : $C_2O_4^{2-}$ Formic acid : $HCOO^-$ Pyrrole (Chlorophyl) : C_4H_5N- etc: $-NH_2$, -NH

Table 3. Linear correlation coefficients (r) of the relationship between stream discharge (Q), the flux of Si, and non-free ionic fractions (NIF) during no rainfall periods. The y-intercept of the correlation line was on the origin because Si does not occur without stream discharge, also implying no NIF production without baseflow discharge. Thus, the coefficient a and b are relatively expressed as $y=ax$ where y is Si and x is Q and $y=bx$ where y is NIF and x is Si.

		Coniferous catchment		Deciduous catchment	
x	y	r	a or b	r	a or b
Q *vs.*	Si	0.99	6.84	0.99	4.93
	NIF-Na	0.93	0.10	0.93	0.21
Si *vs.*	NIF-Mg	0.93	0.05	0.92	0.08
	NIF-Ca	0.96	0.34	0.96	0.50

Table 4. Linear correlation coefficients (*r*) of the relationship between stream discharge (*Q*) and the flux of Si, and non-free ionic fractions (NIF) during the rainfalls. The coefficient *a* and *b* are same as those in Table 3. The *r*-values which exceeded 0.80 (strong correlation) are expressed by the bold style.

(a) Storm 1		Coniferous catchment		Deciduous catchment	
x	*y*	*r*	*a* or *b*	*r*	*a* or *b*
Q *vs.*	Si	**0.90**	6.01	**0.80**	3.89
	NIF-Na	0.79	0.20	0.22	0.25
Si *vs.*	NIF-Mg	**0.89**	0.08	0.69	0.10
	NIF-Ca	0.54	0.15	0.58	0.30

(b) Storm 2		Coniferous catchment		Deciduous catchment	
x	*y*	*r*	*a* or *b*	*r*	*a* or *b*
Q *vs.*	Si	**0.99**	5.82	**0.99**	2.96
	NIF-Na	0.40	0.06	**0.97**	0.25
Si *vs.*	NIF-Mg	0.71	0.08	**0.92**	0.28
	NIF-Ca	0.59	0.30	**0.87**	1.32

Table 5. Linear correlation coefficients (r) of the relationship between the fluxes of fulvic acid like materials (FAM), Si, non-free ionic fractions (NIF), and non-free ionic fractions originated in the baseflow component of stream water (ΔNIF) during the rainstorms; the coefficient c and constant d which are expressed as $y=cx+d$, where y is the Si or NIF and x is FAM. The r-values in the parentheses under $r < 0.70$ in Storm 2 show the linear correlation coefficients during the rising (left) and falling limb (right) of the hydrograph, respectively, and they which exceeded 0.80 (strong correlation) are expressed by the bold style. We were impossible to obtain the r-values between FAM and ΔNIF-Ca in the deciduous catchment in Storm 1, because ΔNIF-Ca, calculated from Equation 6, was mostly 0 mg s^{-1}.

(a) Storm 1

		Coniferous catchment			Deciduous catchment		
x	y	r	c	d	r	c	d
FAM *vs.*	Si	0.26	0.11	3.35	0.51	0.09	2.38
	NIF-Na	0.31	0.04	0.60	0.44	0.04	0.56
	NIF-Mg	0.26	0.01	0.27	0.54	0.02	0.21
	NIF-Ca	0.14	0.02	0.48	0.60	0.11	0.52
	Δ NIF-Na	0.31	0.03	0.23	**0.86**	0.04	-0.03
	Δ NIF-Mg	0.26	0.01	0.25	0.57	0.01	0.01
	Δ NIF-Ca	0.13	0.02	0.35	—	—	—

(b) Storm 2

		Coniferous catchment			Deciduous catchment		
x	y	r	c	d	r	c	d
FAM *vs.*	Si	0.73	0.89	6.69	**0.87**	0.26	2.69
	NIF-Na	0.20 (0.28, -0.52)	0.02	1.42	**0.83**	0.06	1.05
	NIF-Mg	0.65 (0.68, 0.62)	0.06	0.97	**0.97**	0.09	0.25
	NIF-Ca	0.50 (0.50, 0.52)	0.17	4.38	**0.98**	0.42	0.97
	Δ NIF-Na	**0.88**	0.15	-0.32	0.53 (**0.92**, -0.31)	0.01	0.45
	Δ NIF-Mg	**0.81**	0.06	0.59	**0.98**	0.07	0.01
	Δ NIF-Ca	**0.87**	0.15	0.52	**0.99**	0.29	-0.44